Using scanning electrochemical microscopy to examine copper(I) sensitizers for dye sensitized solar cells.

Colin J. Martin[a], Biljana Bozic-Weber[a], Edwin C. Constable[a]*, Thilo Glatzel[b], Catherine E. Housecroft[a] and Iain A. Wright[a]*

[a] Department of Chemistry, University of Basel, Spitalstrasse 51, CH-4056 Basel, Switzerland.

Fax: +41 61 267 1018; Tel: +41 61 267 1001; E-mail: edwin.constable@unibas.ch

[b] *Department of Physics, University of Basel, Klingelbergstrasse 82, CH-4056 Basel, Switzerland.*

Abstract

The examination of surface charges within dye sensitized solar cells (DSCs) containing copper(I)-based dyes has proved to be difficult due to the instability of these systems compared to existing commercial dyes. We report the use of scanning electrochemical microscopy (SECM) in a setup in which homoleptic $[Cu(L_{ancillary})_2]^+$ complexes are used as the electrolyte to investigate a series of $[Cu(L_{anchor})(L_{ancillary})]^+$ sensitizers. The ligands L_{anchor} and $L_{ancillary}$ are 6,6'-disubstituted 2,2'-bipyridines. By incorporating sensitizers and electrolytes containing the same

ligands, changes in the diffusion layer around the scanning electrode have been used to map the substrate surface both in the dark and under controlled illumination. Examination of the changes in current as a constant potential is applied shows the formation of stable surface charge as the cell components equilibrate. Comparison of the time taken for this stabilization to occur as ancillary or anchoring ligands within the dye and electrolyte are varied shows a significant dependence upon the aliphatic substituents in the 6,6'-positions of the ligands which surround the copper(I) center.

Keywords

Scanning electrochemical microscopy.

Dye sensitized solar cell.

Copper(I) sensitizers.

Copper(I)-based electrolytes.

Introduction

Scanning electrochemical microscopy (SECM) is a technique used for the examination of surfaces with high sensitivity at and below the micrometer scale.[1-2] Application of this scanning methodology has resulted in the development of techniques allowing for the investigation of surfaces, both in terms of their topology and their reactivity.[3] Recently, SECM has also been used to investigate photophysical processes on catalytic and reactive surfaces[4-7] and investigations of local activity independent of topology within a catalytic system has been reported.[8] These studies have demonstrated the possibility of monitoring changes in the electronic properties of functionalized semiconducting substrates under variable conditions, with the potential for examining the effect of illumination upon active substrates present at the surface.

In our experimental setup, a non-earthed substrate is submerged in a redox-active electrolyte and an ultramicroelectrode (UME) placed within micrometer distances of the electrically floating surface. The UME is then used as the working electrode in a three electrode electrochemical cell configuration; a potential is applied between the working and reference electrodes and the current flow at the UME is measured. The current flow observed in the diffusion layer around the microelectrode tip is either enhanced or decreased depending upon the conductivity of the substrate surface (Figure 1). In the case of an insulating surface, electron regeneration is hindered, leading to a decrease in current at the microelectrode tip. If, however, the surface is conducting, an enhancement of electron flow occurs and higher currents are measured. These variations can be used to map conductivity by holding the UME at constant distance from the substrate and scanning the surface. Changes in conductivity with respect to distance from the substrate can be used to study the effect of diffusion within the electrolyte.[9] By systematically examining changes in the diffusion layer under irradiation over time, the effect of illumination on photoactive surfaces can also be studied. From this, information about the surface interactions with the electrolyte, as well as sensitizer stability, can be measured.[10]

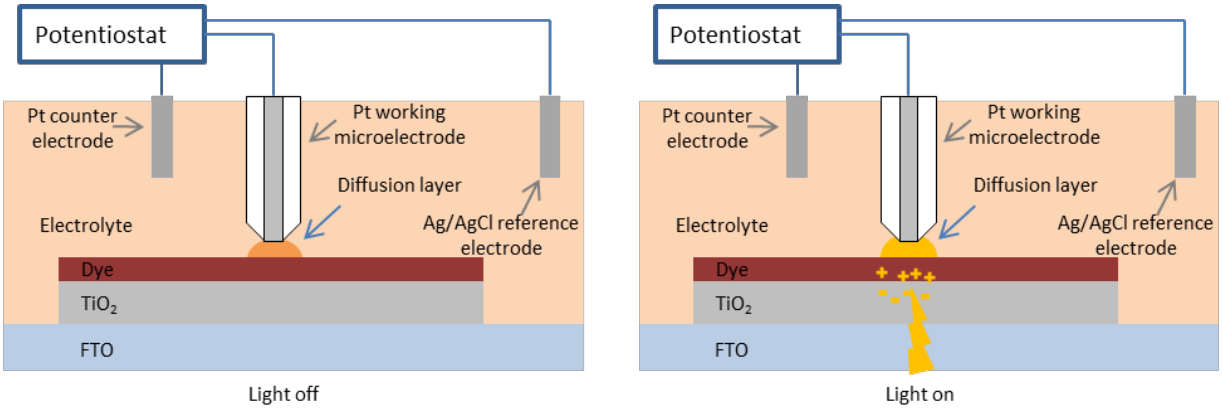

Figure 1. Diagrammatic representation of the changes in diffusion layer observed around the UME tip under light off and on conditions.

Related studies on DSC-SECM setups have shown the complexity of the surface interactions with variations resulting from multiple factors including temperature, viscosity and electrolyte makeup.[10-12] Previously we have described the use of SECM for the study of both charge carrier effects and surface-electrolyte equilibrium in DSCs containing commercially available ruthenium sensitizers.[10,13] We have now extended our investigations to include the characterization of copper(I) sensitizers in DSCs. The application of dyes containing earth abundant metals such as zinc, copper and iron with a view to lowering the cost and environmental impact of device manufacture without sacrificing performance is a topic of considerable interest in modern materials chemistry.[14-17] Copper(I) complexes have been proposed as potential alternatives for use in DSC's because of similarities between their photophysical similarities and those of established ruthenium(II) sensitizers.[18] We have previously discussed the DSC properties of a number of copper(I) dyes in which bis(phosphonic acid) substituted 6,6'-dimethyl-2,2'-bipyridines (6,6'-Me_2bpy) are used as anchoring ligands (L_{anchor}) to tether heteroleptic $[Cu(L_{anchor})(L_{ancillary})]^+$ dyes to titanium dioxide surfaces (Scheme 1). Recently, we reported how changing the steric properties of the substituents in the 6,6'-positions of the ancillary ligand affected the performance of the dye in devices. Of the $[Cu(L_{anchor})(L_{ancillary})]^+$ complexes shown in Scheme 1, the dye with the isobutyl substituents ($L_{ancillary}$ = **3**) gave the best performance.[19] We also confirmed that DSC performance is enhanced by an aromatic spacer in the anchoring ligand.[20] We now present initial investigations into the effect of irradiation on these $[Cu(L_{anchor})(L_{ancillary})]^+$ systems using SECM.

In a standard DSC, a redox active electrolyte is injected between two electrodes (usually made from FTO coated glass), one of which contains dye adsorbed upon a nanoparticulate titanium dioxide (anatase) surface. Upon illumination, power generation occurs as a result of electron

injection from the photo-excited dye into the TiO_2 layer and resultant transport of electrons through the anode to the circuit load. The oxidized dye is reduced by the redox electrolyte in the cell, and the oxidized form of this couple migrates to the cathode where it is regenerated in its reduced form. In the SECM, it is possible to exclusively monitor the interactions between the excited dye and the electrolyte by measuring changes in the effect on the surface as illumination conditions are varied.

In previous DSC-SECM studies, electrolytes including the I^-/I_3^- redox couple have been examined.[8,17] Unlike the commonly employed Ru(II) dyes, the ligands of $[Cu(L_{anchor})(L_{ancillary})]^+$ complexes are labile in solution and in the open cell methods required for SECM studies, interactions with the I^-/I_3^- electrolyte leads to stripping of the sensitizer from the anatase surface. To circumvent this problem, we have used an electrolyte solution in which the homoleptic $[Cu(L_{ancillary})_2]^+$ complex is present. This allows the investigation of the build-up of charge on the unearthed substrate surface while also permitting the complex to undergo ligand exchange with the electrolyte. The latter leads to reformation of the dye. Although this ignores any interactions occurring at the cathodic part of a DSC, it permits the examination of the electronic effects at the anode surface in an innovative and highly revealing manner. Temperature gradient studies showed minimal thermal effects as a result of illumination indicating that only electronic effects are observed within the setup.

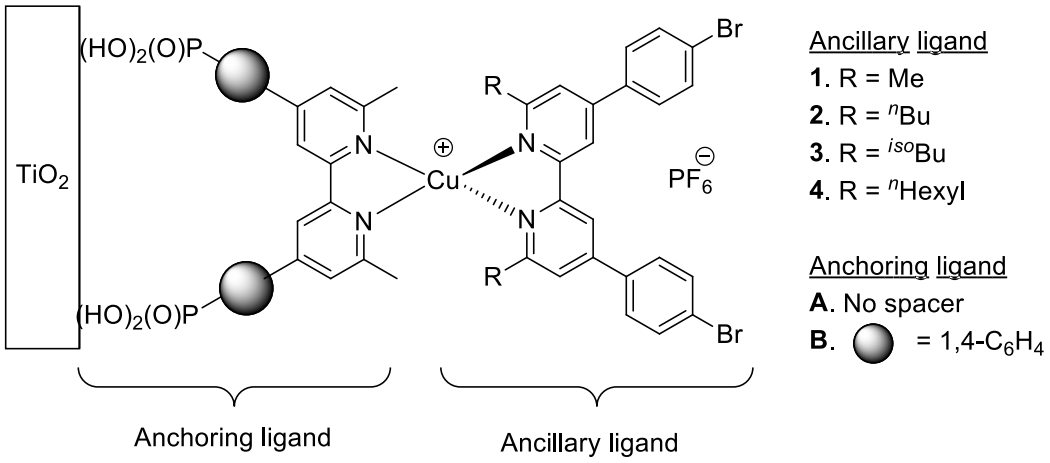

Scheme 1. Schematic representation of the copper(I) sensitizers $[Cu(L_{anchor})(L_{ancillary})][PF_6]$ used in this work.

Experimental section

Anchoring ligands **A** and **B** and homoleptic $[Cu(L_{ancillary})_2][PF_6]$ complexes ($L_{ancillary}$ = **1-4**) were prepared as previously reported.[19] Electrolyte solutions $[Cu(L_{ancillary})_2]^+$ ($L_{ancillary}$ = **1-4**) containing $[Cu(L_{ancillary})_2][PF_6]$ (1 mM) and $[^nBu_4N][PF_6]$ (5 mM) in 3-methoxypropionitrile were prepared.

Substrate preparation TiO_2 paste was prepared adapting the procedure of Grätzel and co-workers;[22] changes to the published procedure were the use of a porcelain (in place of alumina) mortar, sonicator bath in place of an ultrasonic horn, terpineol (CAS: 8000-41-7) rather than α-terpineol, and the omission of the three roller mill treatment. The FTO glass (Solaronix TCO22-7, 2.2 mm thickness, sheet resistance ≈7 Ω square^{-1}) was cleaned by sonicating in acetone, EtOH, Hellmanex® surfactant (2% in water), water and EtOH baths sequentially for 10 min. After treatment in a UV-O_3 system (Model 256-220, Jelight Company Inc.), the FTO plates were immersed in aqueous $TiCl_4$ solution (40 mM) at 70 °C for 30 min, and washed with H_2O and

EtOH. FTO/TiO_2 substrates were made by doctor blading TiO_2 paste[22] onto a conducting glass slide and kept at room temperature for 10 min to allow the paste to mature in order to minimize surface irregularities. The substrate was then gradually heated under an air flow at 70 °C for 30 min, 135 °C for 5 min, 325 °C for 5 min, 375 °C for 5 min, 450 °C for 15 min, and 500 °C for 15 min. After annealing, the TiO_2 film was treated with 40 mM $TiCl_4$ solution as described above, rinsed with H_2O and EtOH and sintered at 500 °C for 30 min. The substrates possessed similar thicknesses and topologies with a thickness of between 11 and 12 μm for all cells. The electrodes were cooled to ca. 80 °C and immersed in a 1 mM DMSO solution of anchoring ligands **A** or **B** for 20 h. The white electrode was removed from the solution, washed with DMSO and EtOH and dried under a stream of N_2. The electrode was then immersed in a 1 mM MeCN solution of $[Cu(L_{ancillary})_2][PF_6]$ ($L_{ancillary}$ = **1**-**4**) for four days to produce red colored electrodes. The electrodes were removed from the solution and washed with CH_2Cl_2 and dried under a stream of N_2.

Cell illumination setup In order to deliver light effectively over a small area of the surface of the substrate, a modified SECM cell in which a controlled light source irradiates part of the dye functionalized surface has been constructed (supplemental information, S1 and S2). A commercially available Thorlabs OSL1-EC halogen lamp source was coupled to Thorlabs BFH48-1000 optical wiring (Ø1 mm core) using an SMA adaptor. This was then placed through a 1.1 mm diameter hole in the bottom of the SECM cell and a circular piece of Laseroptik UV-FS glass (refractive index Na = 0.48) of thickness 6.35 mm placed above it in a custom made Teflon base which fitted into a standard SECM μ-holder. The glass has a cut off range (200-2100 nm) allowing only for light between these wavelengths to affect the substrate surface. Lateral high resolution SECM scans of a test substrate under illumination shows a conical profile of

diameter 4 mm affected by the application of light. This is consistent with the area in which light is expected to be observed based upon the wire core, glass size and refractive index (calculated as 4.2 mm). Calibration at different light intensities was carried out using a Thorlabs PM100 power meter fitted with a Thorlabs model D3MM detector head, to measure the total light hitting the surface. From this the light intensity (per cm^2) was calculated and calibrated relative to the amount of light emitted from the source lamp at different variable settings. Temperature gradients were investigated using a 3-methoxyproponitrile solution of 5 mM $[^nBu_4N][PF_6]$; a Pt-100 resistance thermometer was placed over the point of illumination both in the dark and under illumination at 80 mW cm^{-2}. Multimeter detection of cell resistance was converted to temperature change and in both cases showed an increase of 0.5ºC in the first 5 minutes, attributed to equilibration of the detector head, followed by maintaining a stable temperature for at least one hour (supplemental information, S3).

Electrochemical experiments All SECM was performed with a Uniscan 15 μm Pt UME close to the substrate surface, using a Uniscan M370 SECM operating in feedback mode. The experiments were performed over FTO with a copper dye sensitized TiO_2 layer. UME tips were acid cycled,[23] polished and checked under an optical microscope before use. Before the SECM measurements, the substrate surface was levelled using a Wyler high precision (type 72) circular spirit level and checked by measuring line scans for tilt in both the X and Y directions. Approach curves were run at appropriate potentials, using the desired electrolyte, in small increments (2 μm every 5 seconds) in the dark, until the current reached 50% of the bulk current. For the surface examination, a three electrode setup consisting of a Pt UME working, Pt counter and printed Ag/AgCl reference electrodes was employed.

Results and discussion

We have previously described the synthesis of ancillary ligands **1**-**4** and anchoring ligands **A** and **B** (Scheme 1) for use as sensitizers in DSCs.[19] Each of these ancillary-anchor pairs was prepared *via* anchoring ligand (**A** or **B**) adsorption onto an FTO/TiO_2 surface followed by immersion in a solution containing the homoleptic $[Cu(L_{ancillary})_2][PF_6]$ ($L_{ancillary}$ = **1**-**4**) complex. Depending on the ligands used, this resulted in the formation of the heteroleptic copper(I) complexes $[Cu(\mathbf{A})(L_{ancillary})][PF_6]$ or $[Cu(\mathbf{B})(L_{ancillary})][PF_6]$ with $L_{ancillary}$ = **1**-**4** (Scheme 1) on the surface. Red electrolyte solutions containing a homoleptic $[Cu(L_{ancillary})_2][PF_6]$ complex ($L_{ancillary}$ = **1**-**4**) with a five times excess of $[^nBu_4N][PF_6]$ were prepared. As an initial test of suitability for SECM analysis, optimization of the electrolyte concentrations was carried out. The results showed that absorption of light by the homoleptic $[Cu(L_{ancillary})_2][PF_6]$ complex in solution leads to significant shifts in the background currents around the UME tip. Thus, significantly lower concentrations of redox active electrolyte were required compared to those employed in a conventional DSC setup with an electrolyte such as I^-/I_3^-. It was important, however, to ensure that sufficient electrolyte was present to observe current flow within the SECM cell to allow valid observations. We determined that the optimum electrolyte compositions comprised 1 mM of $[Cu(L_{ancillary})_2][PF_6]$ with 5 mM $[^nBu_4N][PF_6]$. From cyclic voltammetry analysis, this electrolyte composition is stable within the region –0.75 to +0.70 V (*vs*. Ag/AgCl) with irreversible reduction observed below –0.75 V. In solution the copper(I) homoleptic complexes establish a statistical equilibrium with the two heteroleptic complexes and no electrochemical studies have been reported for such systems; however their stability when surface bound has been established within the studied potential region. The potential applied between the working

and reference electrodes for all initial studies was –0.4 V; this was found to support sufficient current to allow for detection of changes resulting from the excitation of dye on the substrate surface at nA levels. The system was calibrated using standard SECM techniques[1] and the tip held 30 μm from the surface. The FTO/TiO_2/sensitizer substrates were irradiated (70 mW cm^{-2} intensity) from underneath and a 6 × 6 mm^2 area of the surface scanned at intervals of 33.3 μm.

Upon excitation of the copper dye on the surface, electron-hole pairs are formed, leading to fast injection of excited electrons into the semiconducting titanium dioxide layer. As a consequence, an excess of holes becomes concentrated at the surface. These can undergo recombination with the redox active electrolyte to reform ground state sensitizers; however the timescale for this process is slower than that of electron injection.[24] Equilibrium is established between the surface charge and the electrolyte as the TiO_2 layer fills with charge injected electrons, leading to a concentration of positive charge at the substrate surface. This can be detected by a working UME close to the surface when the SECM operates under a negative tip potential.

We first consider the sensitizer $[Cu(\mathbf{A})(\mathbf{1})]^+$ containing the 6,6'-dimethyl substituted ancillary ligand **1** and anchoring ligand **A** (Scheme 1). Upon irradiation and scanning at –0.40 V, a conical area of increased current is detected centered on the focal point of irradiation (Figure 2).

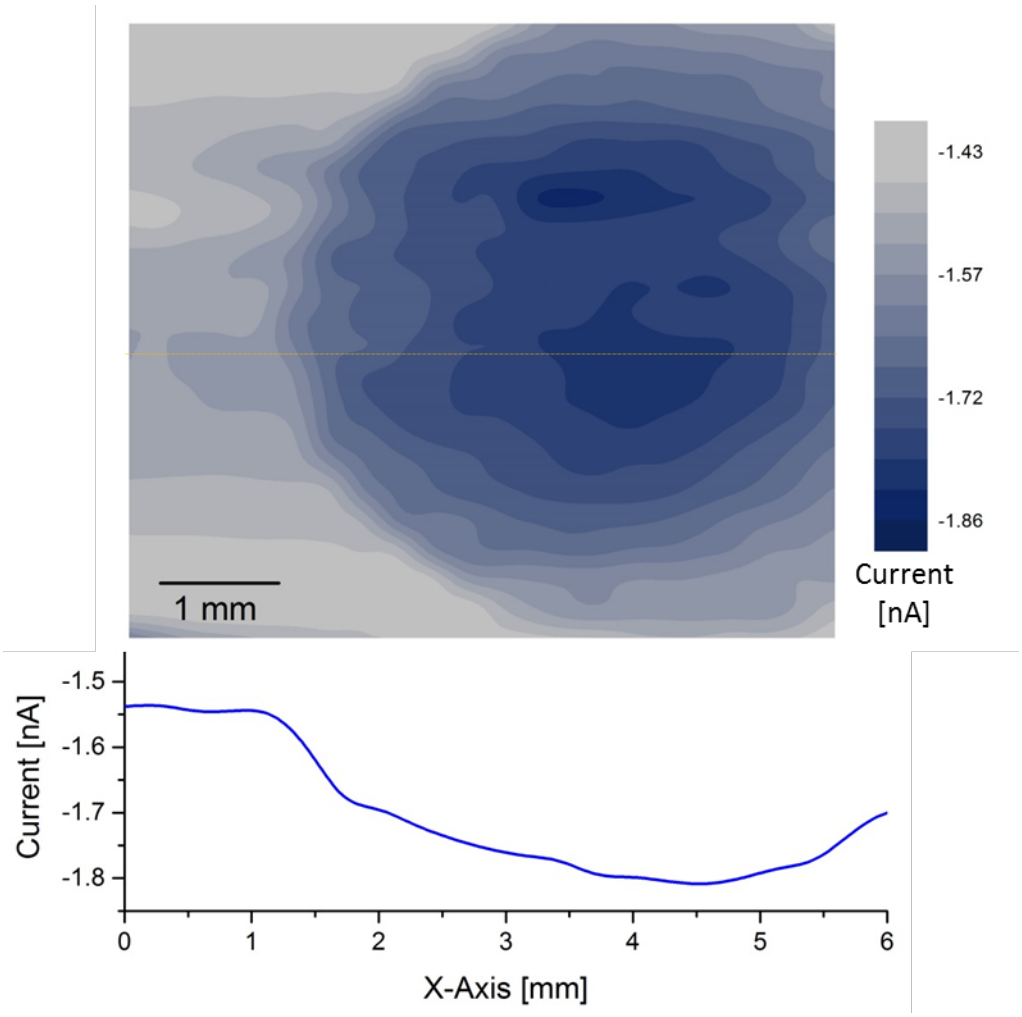

Figure 2. Area and profile scan of a substrate surface of surface-bound [Cu(**A**)(**1**)]$^{+}$ under localized illumination (70 mW cm^{-2}) in the presence of electrolyte [Cu(**1**)$_2$]$^{+}$ scanned under negative tip bias (–0.40 V).

The shape of the contours is due to the fact that light is refracting through the glass under the substrate, resulting in an apex of current at the center of a cone of diameter 4 mm. This is consistent with the area (calculated as having diameter 4.2 mm) in which light is expected to be observed based upon the wire core, glass size and refractive index. For each electrolyte solution, a small shift in current far away from the surface is detected; for the electrolyte solution [Cu(**1**)$_2$]$^{+}$, this is from –1.43 nA in the dark to –1.40 nA under illumination. This results from the

absorption of light leading to some charge separation within the bulk electrolyte and a resultant small variation in redox active species within the diffusion layer of the UME. Similar changes are observed for the other systems with shifts between –0.03 and +0.05 nA.

Given the low current responses observed, we decided to examine the change in current as the UME moves away from the substrate surface by an electrode retraction study. Here, under illumination, the UME was placed above the position of maximum current and then slowly retracted and current measured every 5 μm. The system was first calibrated in the dark *via* an approach curve and as the UME moved to within μm distances of the surface, the predicted fall off in current due to surface-blocked diffusion to the UME was observed for $[Cu(\mathbf{A})(\mathbf{1})]^+$, in the presence of electrolyte $[Cu(1)_2]^+$ (Figure 3a, dotted line); when the current reduced to 50% of the bulk, the UME was assumed to be within 5 μm of the surface.[1] The substrate was then irradiated continuously for 10 minutes in order to maintain stable surface-electrolyte equilibrium. Subsequently the electrode was slowly retracted from the surface while the potential between the working and counter electrodes was held at –0.4 V under continuous illumination of 70 mW cm^{-2} (Figure 3a, dashed line). By subtracting the retraction curve run in the dark from the curve run under illumination and modularizing we obtain an indication of the variation in current response to incident light with respect to increasing distance between the electrode tip and the surface (Figure 3a, solid line). In order to establish the reproducibility of this methodology, a series of retractions at different speeds and retraction distances were carried out in the more responsive I^-/I_3^- electrolyte using the commercially available ruthenium(II) N719 sensitizer (supplemental information S4). Each showed similar current enhancements close to the surface under illumination.

Retraction curves were then measured for each of the four copper sensitizers and corrected with the respective dark retraction data to give the variation curves seen in Figure 3b.

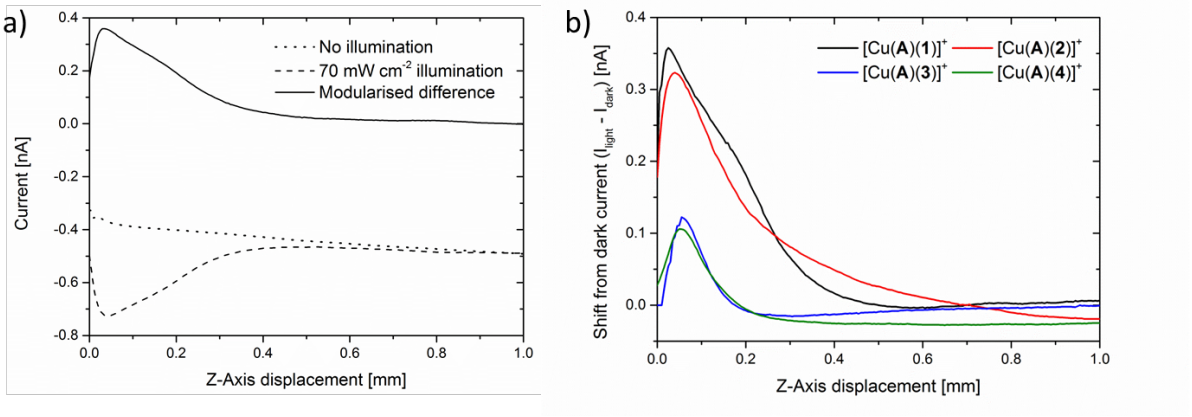

Figure 3. a) Currents in the dark (dotted line) and under illumination at 70 mW cm^{-2} (dashed line) upon retraction from the surface at a tip potential of –0.4 V along with the modularized difference (solid line) for [Cu(**A**)(**1**)]$^+$, in the presence of electrolyte [Cu(**1**)$_2$]$^+$ b) Variations for [Cu(**A**)(**1**)]$^+$, [Cu(**A**)(**2**)]$^+$, [Cu(**A**)(**3**)]$^+$ and [Cu(**A**)(**4**)]$^+$ in the presence of electrolytes [Cu($L_{ancillary}$)$_2$]$^+$ ($L_{ancillary}$ = **1**-**4**).

For the four sensitizers [Cu(**A**)(**1**)]$^+$, [Cu(**A**)(**2**)]$^+$, [Cu(**A**)(**3**)]$^+$ and [Cu(**A**)(**4**)]$^+$ containing the anchoring ligand with no spacer, an area of increased current flow is seen as far as 300 μm from the surface: at distances of 0-30 μm, the current falls off due to the close proximity of the UME. In all cases, an increase in current is seen with a maximum value corresponding to 50-100 μm from the surface. This results from the increased electron flow within the UME diffusion layer due to the charge present at the surface. The intensity of these changes is consistent with those seen in the area scans, with the highest response for the methyl and *n*-butyl containing sensitizers [Cu(**A**)(**1**)]$^+$ and [Cu(**A**)(**2**)]$^+$ respectively. In the case of the isobutyl and *n*-hexyl substituted systems [Cu(**A**)(**3**)]$^+$ and [Cu(**A**)(**4**)]$^+$, a significant decrease in current near the surface compared

to the other sensitizers is observed. This is due to the increased chain bulk which results in lower concentrations of sensitizer on the substrate surface as well as more localized surface charge. It is also worth noting that in all four cases, at distances 1 mm from the surface the effect of electrolyte absorption of light can be seen. This was similar to the changes observed in the area scans, with shifts of between –0.05 and +0.05 nA between the illuminated and dark currents detected as far as 1 mm from the surface for the retraction studies.

We now look at the effect of introducing a spacer into the anchoring ligand (Scheme 1) by comparing the retraction curves for [Cu(**A**)(**2**)]$^+$ and [Cu(**B**)(**2**)]$^+$. The nature of the anchor can have an effect on the dissipation of charge within the electrolyte around it. Taking [Cu(**A**)(**2**)]$^+$ and [Cu(**B**)(**2**)]$^+$ as a representative pair of dyes, the maximum increase in current falls from 0.32 nA in [Cu(**A**)(**2**)]$^+$ to 0.27 nA in [Cu(**B**)(**2**)]$^+$ (Figure 4). However the extended conjugation in anchoring ligand **B** results in an increase in the distance from the surface at which higher concentrations of charge can be observed. This is consistent with the results seen under DSC conditions where the extended charge region close to the surface results in an increase in the short circuit current density and a resultant higher DSC efficiency.[19]

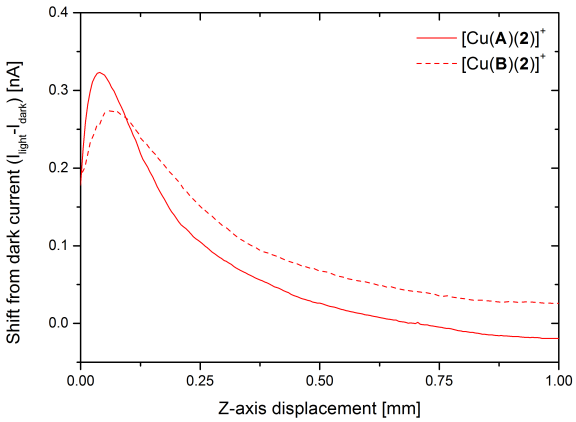

Figure 4. Variation from dark current around the UME tip upon retraction from the surface of $[Cu(\mathbf{A})(\mathbf{2})]^+$ and $[Cu(\mathbf{B})(\mathbf{2})]^+$ in the presence of electrolyte $[Cu(\mathbf{2})_2]^+$, under illumination at 70 mW cm^{-2} at a tip potential of –0.4 V.

Once the optimum configurations for the surface charge-electrolyte equilibrium were known, a chronoamperometric investigation of current under a constant applied potential as light is turned on and off was carried out. Firstly, the tip was placed at a distance within the region of maximum current response to the substrate surface and allowed to equilibrate for 30 minutes at –0.4 V. For each sensitizer-electrolyte pair, the current at the UME was then measured as light (70 mW cm^{-2}) was applied for 30 min and then switched off. In order to establish the reproducibility of this methodology, a series of measurements were first carried out for the more responsive I^-/I_3^- electrolyte using the commercially available N719 sensitizer (supplemental information S5). In all cases these showed values that were reproducible with all computationally fitted half-lives within 10% of each other.

For the copper sensitizers, given the small changes in current involved, each experiment showed some linear drift in current as potential was applied resulting from small variations in the UME tip position over longer time periods. This can best be seen in the case of $[Cu(\mathbf{A})(\mathbf{4})]^+$ in which the relative drift observed is largest (Figure 5, red). This was corrected by computationally

fitting the linear drift after the system has stabilized under illumination (Figure 5, dashed blue line) and subtracting it from the data, leaving only the changes in current resulting from the surface-electrolyte interactions (Figure 5, black).

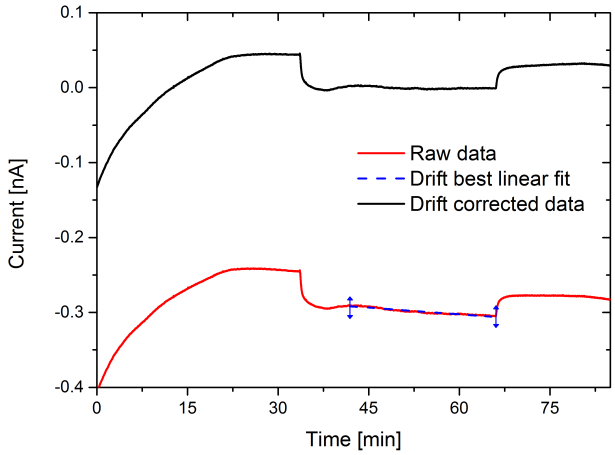

Figure 5. Raw data, computationally fitted drift and drift corrected changes in current at the surface of sensitizer [Cu(**A**)(**4**)]$^{+}$ in the presence of electrolyte [Cu(**4**)$_2$]$^{+}$ (irradiation 70 mW cm^{-2}, scans run at –0.40 V bias).

This correction also allows for easier comparison of different setups as it sets the current with light on to a value of 0 nA. To allow for clearer comparison of the four systems, the time scales were also corrected relative to the instant of initial light variation. Comparing the light on/off chronoamperometry for the four non-spaced anchor systems [Cu(**A**)(**1**)]$^{+}$ to [Cu(**A**)(**4**)]$^{+}$ three features are observed in each (Figure 6).

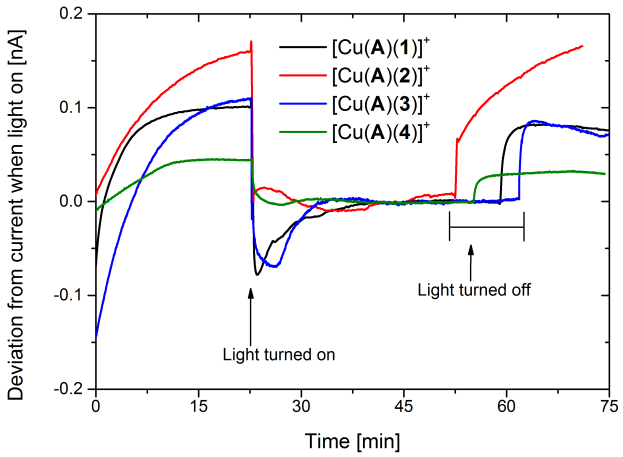

Figure 6. Changes in current at the surface of $[Cu(\mathbf{A})(\mathbf{1})]^+$, $[Cu(\mathbf{A})(\mathbf{2})]^+$, $[Cu(\mathbf{A})(\mathbf{3})]^+$ and $[Cu(\mathbf{A})(\mathbf{4})]^+$ substrates as light is turned on and off in the presence of electrolytes $[Cu(L_{ancillary})_2]^+$ ($L_{ancillary}$ = **1**-**4**), corrected for linear drift (irradiation 70 mW cm^{-2}, scans run at –0.40 V bias).

Initially when the potential is applied in the dark, a slow increase in current is observed. This is similar for three of the dye/electrolyte combinations, with exponentially fitted half-lives between 219 - 361 s determined for $[Cu(\mathbf{A})(\mathbf{1})]^+/[Cu(\mathbf{1})_2]^+$, $[Cu(\mathbf{A})(\mathbf{3})]^+/[Cu(\mathbf{3})_2]^+$ and $[Cu(\mathbf{A})(\mathbf{4})]^+/[Cu(\mathbf{4})_2]^+$ (Table 1). As these are dark conditions, these values depend only upon the electrolyte, with stabilization of the charge taking the shortest time for the least sterically hindered electrolyte $[Cu(\mathbf{1})_2]^+$. In the case of $[Cu(\mathbf{A})(\mathbf{2})]^+/[Cu(\mathbf{2})_2]^+$ which contains the *n*-butyl substituents, a longer half-life of 583 s was determined. This is attributed to the instability of this system under constant applied potential which results in the formation of doped degradation products on the UME and the subsequent lack of clear exponential variations as light is turned on or off.

Table 1. Fitted half-lives (error +/- 10%) for chronoamperometric variations close to sensitized substrate surfaces as light is turned on and off in the presence of electrolytes $[Cu(L_{ancillary})_2]^+$

($L_{ancillary}$ = **1**-**4**), after correction for linear drift (irradiation 70 mW cm^{-2}, scans run at –0.40 V bias).

Dye/electrolyte pair	Initial half life [s]	Light on time to maximum [s]	Light on half life [s]	Light off half life [s]
$[Cu(\mathbf{A})(\mathbf{1})]^+$/ $[Cu(\mathbf{1})_2]^+$	219	48	333	51
$[Cu(\mathbf{A})(\mathbf{2})]^+$/ $[Cu(\mathbf{2})_2]^+$	583	-	-	-
$[Cu(\mathbf{A})(\mathbf{3})]^+$/ $[Cu(\mathbf{3})_2]^+$	361	196	117	23
$[Cu(\mathbf{A})(\mathbf{4})]^+$/ $[Cu(\mathbf{4})_2]^+$	320	272	116	70

In all cases an increase in negative current is observed upon irradiation (Figure 6); for three of the sensitizers this reaches a maximum which then decays leaving a stable current. The speed at which this maximum is reached depends on the 6,6'-substituents in the ancillary ligand. The fastest time is observed for the least sterically hindered system $[Cu(\mathbf{A})(\mathbf{1})]^+/[Cu(1)(\mathbf{2})]^+$ with a maximum reached within 48 seconds. For the isobutyl system $[Cu(\mathbf{A})(\mathbf{3})]^+/[Cu(\mathbf{3})(\mathbf{2})]^+$, the maximum is reached after 196 s and for $[Cu(\mathbf{A})(\mathbf{4})]^+/[Cu(\mathbf{4})_2]^+$ which contains the *n*-hexyl substituents, it takes 272 s. This indicates that the longer the alkyl chains (which envelop the copper(I) center) the longer it takes for the charged titanium dioxide layer to reach equilibrium with the electrolyte. Upon reaching this maximum, the dye/electrolyte systems stabilize to a constant current with the substituent chain length again affecting the half-lives. In the systems with the isobutyl and *n*-hexyl chains the current stabilizes in approximately the same timeframe, while the less encumbered methyl-substituted system takes nearly three times as long (Table 1). This indicates that once a maximum is reached the system becomes stable in a shorter period of time if more sterically demanding alkyl substituents are present.

When light is turned off (Figure 6) the $[Cu(\mathbf{A})(\mathbf{2})]^+/[Cu(\mathbf{2})_2]^+$ system with the *n*-butyl substituents appears distinct from the other systems. It exhibits a much slower change in current, again indicating the formation of doped degradation products on the UME. For the other three

systems (with ligands **1**, **3** and **4**), a slow exponential decay of charge occurs, indicating recombination between the electrolyte and the charged surface as charge is removed from the surface. Here the fastest decay is seen for the isobutyl system with a half-life of 23 s compared to 51 s for the methyl and 70 s for the *n*-hexyl systems. These decay half-lives are similar to those we have reported for other electrolyte-dye systems within DSC-SECM experiments where in all cases current has fallen off within 600 s.[10]

A comparison of the changes in current upon illumination for a set of sensitizers [Cu(**A**)(**3**)]$^+$ and [Cu(**B**)(**3**)]$^+$ in which the ancillary ligand remains the same and the anchoring ligand is changed, shows that the time taken to reach maximum current is much faster when a spacer is present in the anchoring ligand. It takes 5 s for the system containing [Cu(**B**)(**3**)]$^+$ to reach a maximum compared to 196 s for [Cu(**A**)(**3**)]$^+$ (Figure 7).

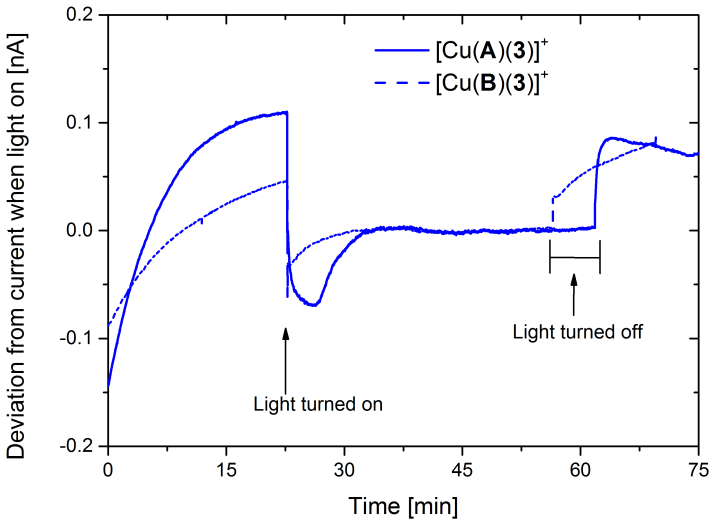

Figure 7. Changes in current at the surface of [Cu(**A**)(**3**)]$^+$ (solid) and [Cu(**B**)(**3**)]$^+$ (dashed) substrates as light is turned on and off in the presence of electrolyte [Cu(**3**)$_2$]$^+$, corrected for linear drift (irradiation 70 mW cm^{-2}, scans run at –0.40 V bias).

This indicates the presence of a longer lived excited state in the spaced anchor, leading to faster charge injection into the titanium dioxide layer. Upon continuous illumination $[Cu(\mathbf{B})(\mathbf{3})]^+$ takes a longer time to equilibrate than was seen using the unspaced anchor (164 s, compared to 117 s for $[Cu(\mathbf{B})(\mathbf{3})]^+$); however given the faster time taken to reach maximum current both setups level off within similar timeframes.

Conclusion

SECM has been used to investigate homoleptic copper(I) electrolytes combined with heteroleptic copper(I)-based sensitizers for DSC applications. By utilizing homoleptic $[Cu(L_{ancillary})_2]^+$ complexes that contain the same ligands as the heteroleptic sensitizers $[Cu(L_{anchor})(L_{ancillary})]^+$, it has been possible to examine the equilibrium between the charge on the substrate surface and the electrolyte under illumination and to map changes in the diffusion layer. All the ligands are derivatives of 2,2'-bipyridine, and the effects of introducing (i) 6,6'-substituents with different steric demands into $L_{ancillary}$, and (ii) an arene spacer into L_{anchor} have been examined. Changes observed close to the surface resulting from equilibrium with photo-generated charge and further away from the surface due to electrolyte absorption of light have been measured as the SECM tip is retracted from the surface.

Looking at the changes in current with time when the UME tip is close to the surface and illumination varied has allowed for the comparison of half-lives for stabilization of the systems and the dependence of stability times on both the anchoring and ancillary ligands. These techniques have been applied to a series of four sensitizers containing different aliphatic chains within the metal coordination sphere and indicate a significant current dependence on the aliphatic chain present.

Acknowledgements

We thank the European Research Council (Advanced Grant 267816 LiLo), the Swiss National Science Foundation, the Nano Argovia programme of the Swiss Nanonscience Institute and the University of Basel for financial support. Sven Y. Brauchli and Frederik J. Malzner are thanked for assistance with complex preparation.

Supporting information

Images of the modified SECM cell base and SECM setup, thermal gradient tests, retraction and chronoamperometric reference scans. This material is available free of charge via the Internet at XXX.

References

[1] Bard, A. J.; Fan, F. R. F.; Kwak, J.; Lev O. Scanning electrochemical microscopy. Introduction and principles. *Anal. Chem.* **1989**, *61*, 132-138.

[2] Amemiya, S.; Bard, A.J.; Fan, F.R.F.; Mirkin, M.V.; Unwin, P.R. Scanning Electrochemical Microscopy, *Annu. Rev. Anal. Chem.* **2008**, *1*, 95-131.

[3] Ballesteros Katemann, B.; Schulte, A.; Schuhmann, W. Constant-distance mode scanning electrochemical microscopy (SECM). Part II: High-Resolution SECM Imaging Employing Pt Nanoelectrodes as Miniaturized Scanning Probes, *Electroanalysis*, **2004**, *16*, 60-65.

[4] Shen, Y.; Tefashe, U.M.; Nonomura, K.; Loewenstein, T.; Schlettwein. D,; Wittstock, G. Photoelectrochemical kinetics of eosin Y-sensitized zinc oxide films investigated by scanning

electrochemical microscopy under illumination with different LED, *Electrochim. Acta* **2009**, *55,* 458-464.

[5] Tefashe, U.M.; Loewenstein, T.; Miura, H.; Schlettwein, D.; Wittstock, G.; Scanning electrochemical microscope studies of dye regeneration in indoline (D149)-sensitized ZnO photoelectrochemical cells. *J. Electroanal. Chem.* **2010**, *650*, 24-30.

[6] Fernández, J.L.; Walsh, D.A.; Bard, A.J. Thermodynamic Guidelines for the Design of Bimetallic Catalysts for Oxygen Electroreduction and Rapid Screening by Scanning Electrochemical Microscopy. M–co (M: Pd, Ag, Au). *J. Am. Chem. Soc.* **2005**, *127*, 357-365.

[7] Barker, A.; Unwin, P.; Zhang, J. Measurement of the forward and back rate constants for electron transfer at the interface between two immiscible electrolyte solutions using scanning electrochemical microscopy (SECM): Theory and experiment, *Electrochem. Commun.* **2001**, *3,* 372-378.[8] Nebel, M.; Erichsen, T.; Schuhmann, W. Constant-distance mode SECM as a tool to visualize local electrocatalytic activity of oxygen reduction catalysts, *Beilstein J. Nanotechnol.* **2014**, *5*, 141–151.

[9] Nicholson, P.G.; Zhou, S.; Hinds, G.; Wain, A.J.; Turnbull, A. Electrochatalytic activity mapping of model fuel cell catalyst films using scanning electrochemical microscopy, *Electrochim. Acta.* **2009**, *54*, 4525-4533.

[10] Martin, C.J.; Bozic-Weber, B.; Constable, E.C.; Glatzel, T.; Housecroft C.E.; Wright I.A. Development of scanning electrochemical microscopy (SECM) techniques for the optimization of dye sensitized solar cells. *Electrochim. Acta.* **2014**, *119*, 86-91.

[11] Schäfer, D.; Puschhof, A.; Schuhmann, W. Scanning electrochemical microscopy at variable temperatures, *Phys Chem Chem Phys*. **2013**, *14*, 5215-5223.

[12] Ejigu, A.; Lovelock, K.R.J.; Licence, P.; Walsh, D.A. Iodide/triiodide electrochemistry in ionic liquids: Effect of viscosity on mass transport, voltammetry and scanning electrochemical microscopy. *Electrochimica Acta*. **2011**, *56*, 10313–10320

[13] Bozic, B.; Figgemeier, E. Scanning electrochemical microscopy under illumination: an elegant tool to directly determine the mobility of charge carriers within dye-sensitized nano structured semiconductors, *Chem. Commun*. **2006**, 2268-2270.

[14] Polo, A.S.; Itokazu, M.K.; Iha, N.Y.M.; Metal complex sensitizers in dye-sensitized solar cells, *Coord. Chem. Rev*. **2004**, *248*, 1343-1361.

[15] Robertson N. Cu^{I} versus Ru^{II}: Dye-Sensitized Solar Cells and Beyond. *ChemSusChem*, **2008**, *1*, 977-979.

[16] Alonso-Vante, N.; Nierengarten J.; Sauvage J. Spectral Sensitization of Large-band-gap Semiconductors (Thin Films and Ceramics) by a Carboxylated Bis(1,10-Phenanthroline) copper(l) Complex. *J. Chem. Soc. Dalton Trans*. **1994**, 1649-1654.

[17] Bozic-Weber, B.; Constable, E.C.; Housecroft, C.E. Light harvesting with Earth abundant d-block metals: towards a sustainable materials chemistry. *Coord. Chem. Rev*. **2013**, *257*, 3089-3106.

[18] Bessho, T.; Constable, E.C.; Graetzel, M.; Hernandez Redondo, A.; Housecroft, C.E.; Kylberg, W.; Nazeeruddin, Md.K.; Neuburger, M.; Schaffner, S. An element of surprise - efficient copper-functionalized dye-sensitized solar cells. *Chem. Commun*. **2008**, *32*, 3717-3719.

[19] Bozic-Weber, B.; Brauchli, S.Y.; Constable, E.C.; Fürer, S.O.; Housecroft, C.E.; Malzner, F.J.; Wright, I.A.; Zampese, J.A. Improving the photoresponse of copper(I) dyes in dye-sensitized solar cells by tuning ancillary and anchoring ligand modules, *Dalton Trans*. **2013**, *42* 12293-12308.

[20] Bozic-Weber, B.; Brauchli, S.Y.; Constable, E.C.; Fürer, S.O.; Housecroft, C.E.; Wright, I.A. Hole-transport functionalised copper(I) dye sensitizes solar cells. *Phys*. *Chem*. *Chem*. *Phys*. **2013**, *15*, 4500-4504.

[21] Kylberg, W.; Wain, A.; Castro, F. Screening of photoactive dyes on TiO_2 surfaces using scanning electrochemical microscopy, *J*. *Phys*. *Chem*. *C* **2012**, *116*, 17384-17392.

[22] Ito, S.; Murakami, T.N.; Comte, P.; Liska, P.; Grätzel, C.; Nazeeruddin, M.K.; Grätzel, M. Fabrication of thin film dye sensitized solar cells with solar to electric power conversion efficiency over 10%, *Thin Solid Films* **2008**, *516*, 4613-4619.

[23] Fushimi, K.; Seo, M. An SECM observation of dissolution distribution of ferrous or ferric ion from a polycrystalline iron electrode, *Electrochim*. *Acta*, **2001**, *47*, 121-127.

[24] Hagfeldt, A.; Boschloo, G.; Sun, L.; Kloo, L.; Pettersson, H. Dye-Sensitized Solar Cells. *Chem*. *Rev*. **2010**, *110*, 6595–6663.

TOC Image